Measurement 253 (2025) 117680

Contents lists available at ScienceDirect

Measurement

journal homepage: www.elsevier.com/locate/measurement

The spectral parametrization of a SEM imaged nanoparticle monolayer

Paweł Weroński

Jerzy Haber Institute of Catalysis and Surface Chemistry, Polish Academy of Sciences, Niezapominajek 8, PL 30239, Krakow, Poland

ARTICLE INFO

Keywords:
Particle image analysis
2D random packing
Static structure factor
Total-correlation function
Finite size effect
Random sequential adsorption
Hard sphere

ABSTRACT

The analysis of computer-generated particle-monolayer images, presented in Measurement 241 (2025) 115692, shows that the novel method of monolayer parametrization described in that paper is insensitive to distortions in apparent particle size. In this short communication, we demonstrate on a SEM micrograph published in the literature that this feature is also preserved in the case of real, imperfect microscopic images of sputter-coated particle monolayers. For this purpose, we use the micrograph to make four images at different degrees of distortion in apparent particle size. Least-squares fitting performed for the four images reveals that the differences in the determined particle size and surface coverage are statistically insignificant. One-way ANOVA performed on the four data sets shows that their means are statistically equal. The Pearson correlation coefficients calculated for the six pairs of the four data sets indicate a strong linear relationship between the sets.

1. Introduction

Particles in the nanometer size range are garnering more attention as interest in nanotechnology continues to grow. They have found many applications in processing and engineering industries, e.g., electronics, oil and gas, cosmetic, and agriculture, with the global nanomaterials market expected to reach US$15.9 billion in 2025 [1]. Nanoparticles play a major role in catalysis [2] and biomedicine [3]. They posses distinct chemical and physical attributes that make them ideal scafolds for creating innovative chemical and biological sensors [4]. The rapid development of electronics makes these devices very cheap and widely available [5].

The production of good quality nanomaterials requires appropriate control of the size and shape of the nanoparticles used. The commonly employed techniques for this purpose are those based on particle-monolayer image-analysis [6–13]. They are non-invasive and cheap, but their application is limited because of the methodology grounded in individual-particle identification. This becomes particularly challenging in dense, tightly packed monolayers or systems with clustered particles [14]. Furthermore, as the number of particles per frame increases, the computational demands rise, especially for methods that utilize machine learning.

Another, indirect method for addressing this issue involves fitting particle-monolayer parameters to the ratio of the discrete power spectral densities (PSDs) computed from the images of the entire monolayer and its individual particle [15]. This approach is especially attractive today, as many software packages for image analysis provide all the essential tools and procedures. Recent findings indicate that the novel strategy not only effectively avoids the need for identifying individual particlesis but can also be insensitive to distortions in apparent particle size [16]. The latter, so far demonstrated for computer-generated particle-monolayer images only, would make the new approach particularly advantageous for parametrizing micrographs of monolayers with distorted apparent particle size. These distortions frequently occur, e.g., in SEM images of sputter-coated monolayers of non-conducting particles or particles on non-conducting substrates. Unlike idealized computer-generated images, real SEM micrographs are influenced by several factors that can distort particle appearance, including noise, contrast variation, and coating effects. Specifically, SEM images are subject to random fluctuations in pixel intensity, variations in local contrast due to differences in particle coating or material properties, and resolution limitations. Additionally, the sputter-coating process introduces further distortions by altering the particle surfaces. In this paper, on the example of a SEM micrograph published in the literature [17], we demonstrate that the feature is preserved also in the case of real, imperfect microscopic images, confirming the robustness of the PSD-based method for handling such distortions.

2. Theoretical considerations

Let us consider a square micrograph of a statistically isotropic monolayer of randomly distributed, spherical, monodisperse particles. We assume the particles do not overlap and the layer is statistically homogeneous. The image is also assumed to be grayscale with a black background, where pixel brightness corresponds to grayscale intensity—i.e., lower values represent darker regions (black = 0) and higher values

E-mail address: ncwerons@cyf-kr.edu.pl.

https://doi.org/10.1016/j.measurement.2025.117680
Received 28 October 2024; Received in revised form 16 April 2025; Accepted 23 April 2025
Available online 5 May 2025

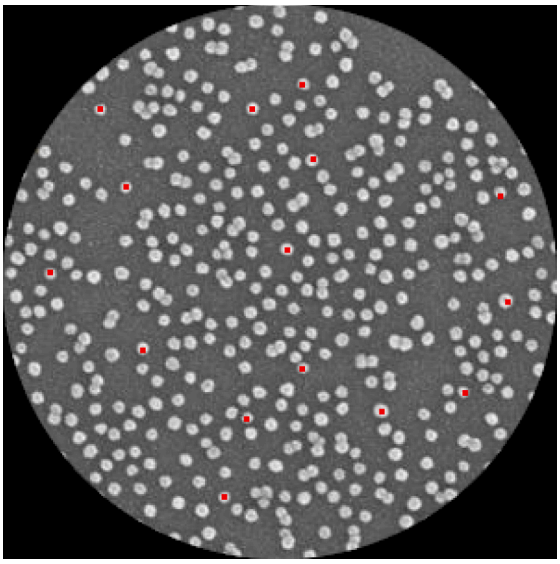

(a) A circular fragment of the original micrograph [17]. Red squares mark the particles used for calculating single-particle PSDs.

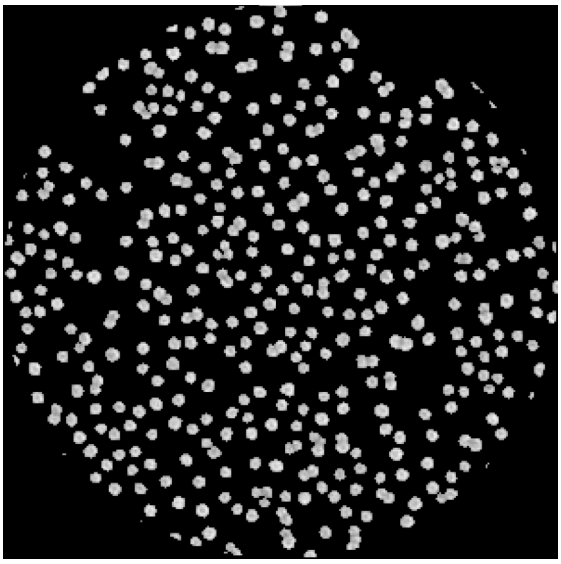

(b) Image S_1 derived from (a) by resetting the pixels of brightness below 141.

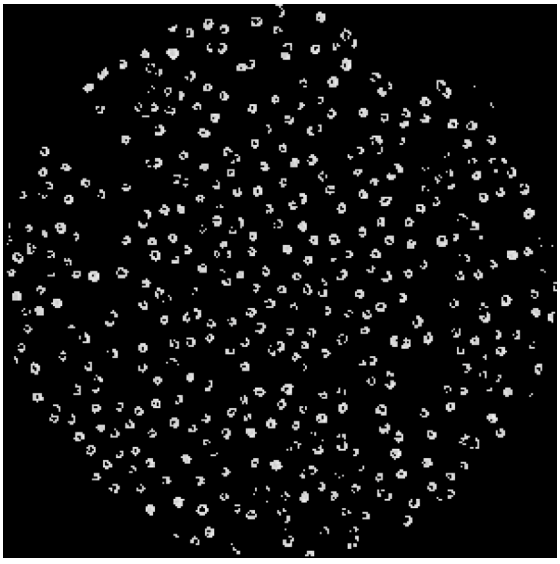

(c) Image S_4 derived from (a) by resetting the pixels of brightness below 201.

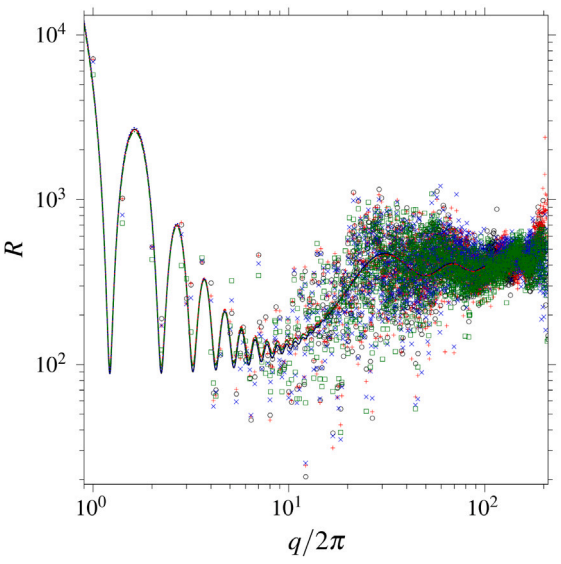

(d) A comparison of the PSD quotients calculated for the four images S_1 to S_4 derived from (a).

Fig. 1. The PSD quotients calculated for four images derived from the same SEM micrograph. (a) A circular fragment of the original micrograph. (b) Image S_1. (c) Image S_4. (d) A comparison of the PSD quotients from the four images S_1 to S_4. Points and lines represent the discrete data derived from FFT and fits to Eq. (1), respectively. Black 'o's and solid line, red '+'s and dash line, blue 'x's and dot line, and green '□'s and dash–dot line denote results for the images S_1, S_2, S_3, and S_4, respectively.

represent brighter regions (white = 255). If color micrographs are used, an appropriate transformation from color to grayscale may be necessary. To achieve isotropy in the monolayer image, we reset all pixels that are more than half the length of the square's side away from its center, effectively limiting the image to a circular fragment inscribed within the black square. Please note that, unless stated otherwise, all dimensional quantities are scaled by appropriate powers of the diameter of the circular fragment.

By utilizing a software package for computing the fast Fourier transform (FFT), we can calculate the discrete PSD of the monolayer image and, after excluding all particles except one, the discrete PSD of the individual particle. Then, we can find the ratio of the two PSDs, $R(q)$, where q denotes the wavenumber. Formal analysis shows that, for a monolayer composed of N particles, the ratio is equal to [15,16]

$$R(qa,\theta,a) = \frac{\theta}{4a^2} S(qa,\theta,a), \tag{1}$$

where a is the dimensionless particle radius, qa is the wavenumber normalized by the particle radius, $\theta = 4Na^2$ is the surface coverage, and

$$S(qa,\theta,a) = 1 + 4\theta \left[\frac{J_1(qa/2a)}{qa}\right]^2 + 2\theta K_c(qa,\theta,a) \tag{2}$$

is the static structure factor. Here, $J_1(x)$ denotes the first order Bessel function of the first kind and $K_c(qa,\theta,a)$ is the Fourier transform of the total correlation function on a finite-size circular area. Usually, for a given type of particle monolayers, this function has to be computed numerically.

If the function $K_c(qa,\theta,a)$ corresponds to the structure of the imaged particle monolayer, Eq. (1) allows to least-squares fit the particle radius and surface coverage of the monolayer. We use the equation to determine the monolayer parameters from four images derived from the same SEM micrograph.

3. Results and discussion

Fig. 1(a) presents a circular fragment of the original micrograph published in Fig. S12b of Ref. [17], of 299 × 299 pixels, which we use to produce four images of the monolayer. The monolayer was formed of gold nanoparticles with a diameter of $24.4\,\mathrm{nm} \pm 3.5\,\mathrm{nm}$, as determined by DLS and TEM. The particles were adsorbed on a silanized glass substrate and sputter-coated for SEM. The monolayer structure resembles that of a hard-sphere RSA system [18], so we can fit the monolayer parameters using the function $K_c(qa, \theta, a)$ calculated for this type of monolayers [16].

First, we produce four grayscale images $S_i\,(i = 1, \ldots, 4)$ of the monolayer by applying different thresholds to the pixel brightness (grayscale intensity). Specifically, all pixels with grayscale values below 141, 161, 181, and 201 are reset to the background value in S_1 through S_4, respectively. Since pixel brightness corresponds to grayscale intensity (with 0 = black and 255 = white), increasing the threshold removes progressively more of the darker pixels, simulating apparent particle size distortion. Figs. 1(b) and 1(c) show the thresholded images S_1 and S_4, corresponding to the lowest and highest cutoff values. For each of the four images S_i, we save 15 images of the single particles marked in Fig. 1(a), calculate their PSDs, and average over them to get four single-particle PSDs $C_{0i}(q)$. Next, we calculate the PSDs $C_i(q)$ of the four monolayer images and divide them by the corresponding single-particle PSDs to get four discrete functions $R_i(q) = C_i(q)/C_{0i}(q)$. Finally, for each of the discrete functions, we determine the parameters a_i and θ_i by least-squares fitting Eq. (1) to the log transformed discrete data.

Specifically, the best-fit parameters and standard deviations are following: $a_1 = (1.374 \pm 0.019) \times 10^{-2}$ and $\theta_1 = 0.2901 \pm 0.0082$, $a_2 = (1.34 \pm 0.02) \times 10^{-2}$ and $\theta_2 = 0.274 \pm 0.009$, $a_3 = (1.37 \pm 0.02) \times 10^{-2}$ and $\theta_3 = 0.291 \pm 0.009$, $a_4 = (1.35 \pm 0.02) \times 10^{-2}$ and $\theta_4 = 0.2752 \pm 0.0081$. Thus, for each pair of $i, j = 1, \ldots, 4$, the standard deviations of a_i and a_j overlap, as do the standard deviations of θ_i and θ_j. This suggests that the differences in the determined particle size and surface coverage are statistically insignificant. The conclusion is also supported by the very small differences between the continuous PSD quotients calculated using Eq. (1) for the fitted values of a_i and θ_i, as presented in Fig. 1(d). Please note that, contrary to theoretical predictions, the discrete values of $R_i(q)$ in the range $q > 100$ do not converge to zero, so we reject them from the fitting procedure.

To confirm the statistical equivalence of the four functions $R_i(q)$, we test their means and linear correlations. The four sets of function values R_i are well approximated by normal distributions with similar variances, so we compare their means using one-way ANOVA. The test shows that the means are statistically equal ($F(3, 4484) = 0.563, p > 0.639$). The Pearson correlation coefficients calculated for the six pairs of the four data sets, which range from 0.887 to 0.962, indicate a strong linear relationship among the sets.

This robustness suggests that the PSD-based parameters extracted from SEM micrographs – particularly the dimensionless particle radius and surface coverage – can be reliably used in broader particle characterization tasks. For example, after appropriate scaling, the estimated radius may be employed to derive absolute particle size relevant to material formulation, quality control, or predictive modeling. Similarly, accurate surface coverage data can support the analysis of packing density, particle interactions, or the interpretation of macroscopic properties such as optical reflectivity or mechanical strength. The method's resilience to image distortion thus reinforces its practical value in experimental workflows where image quality cannot always be guaranteed.

4. Conclusion

The differences in fitting parameters determined for four images of different degrees of distortion in apparent particle size, derived from the same SEM micrograph, are statistically insignificant. There is a strong linear correlation between the investigated PSD quotients. Their means are statistically equal. This suggests that the effect of distortion in apparent particle size—frequently occurring in SEM images—on the fitting monolayer parameters is insignificant.

Declaration of competing interest

The authors declare that they have no known competing financial interests or personal relationships that could have appeared to influence the work reported in this paper.

Acknowledgments

This work has been supported by the statutory funds of ICSC PAS.

Data availability

Data will be made available on request.

References

[1] C. Martin, A. Nourian, M. Babaie, G.G. Nasr, Environmental, health and safety assessment of nanoparticle application in drilling mud – Review, Geoenergy Sci. Eng. 226 (2023) 211767.
[2] C. Xie, Z. Niu, D. Kim, M. Li, P. Yang, Surface and interface control in nanoparticle catalysis, Chem. Rev. 120 (2) (2020) 1184–1249.
[3] B. Rezaei, A. Harun, X. Wu, P.R. Iyer, S. Mostufa, S. Ciannella, I.H. Karampelas, J. Chalmers, I. Srivastava, J. Gómez-Pastora, K. Wu, Effect of polymer and cell membrane coatings on theranostic applications of nanoparticles: A review, Adv. Heal. Mater. n/a (n/a) (2024) 2401213.
[4] K. Saha, S.S. Agasti, C. Kim, X. Li, V.M. Rotello, Gold nanoparticles in chemical and biological sensing, Chem. Rev. 112 (5) (2012) 2739–2779.
[5] O. Riabchenko, O. Kukla, O. Fedchenko, Yu.M. Shirshov, Z. Kazantseva, SPR chromatic sensor with colorimetric registration for detection of gas molecules, SPQEO 26 (3) (2023) 343–351.
[6] G. Köllensperger, G. Friedbacher, M. Grasserbauer, L. Dorffner, Investigation of aerosol particles by atomic force microscopy, Fresenius' J. Anal. Chem. 358 (1–2) (1997) 268–273.
[7] M.K. Francis, R.V. Calabrese, S. Phongikaroon, Novel probe for the in situ measurement of particle size distributions, Rev. Sci. Instrum. 77 (12) (2006) 123704.
[8] G. Milne, Y. Zhao, D.T. Chiu, High-precision measurement and analysis of colloidal monolayers, Anal. Chem. 82 (9) (2010) 3943–3949.
[9] J. Garnaes, Diameter measurements of polystyrene particles with atomic force microscopy, Meas. Sci. Technol. 22 (9) (2011) 094001.
[10] O. Couteau, G. Roebben, Measurement of the size of spherical nanoparticles by means of atomic force microscopy, Meas. Sci. Technol. 22 (6) (2011) 065101.
[11] T. Klein, E. Buhr, K.P. Johnsen, C.G. Frase, Traceable measurement of nanoparticle size using a scanning electron microscope in transmission mode (TSEM), Meas. Sci. Technol. 22 (9) (2011) 094002.
[12] M.J. McDonald, A. Yethiraj, L.Y. Beaulieu, A method to characterize structure and symmetry in low-resolution images of colloidal thin films, Meas. Sci. Technol. 23 (4) (2012) 045606.
[13] S.B. Rice, C. Chan, S.C. Brown, P. Eschbach, L. Han, D.S. Ensor, A.B. Stefaniak, J. Bonevich, A.E. Vladár, A.R. Walker, J. Zheng, C. Starnes, A. Stromberg, J. Ye, E.A. Grulke, Particle size distributions by transmission electron microscopy: An interlaboratory comparison case study, Metrologia 50 (6) (2013) 663–678.
[14] J. Li, S. Shao, J. Hong, Machine learning shadowgraph for particle size and shape characterization, Meas. Sci. Technol. 32 (1) (2021) 015406.
[15] P. Weroński, K. Pałka, Roughness spectroscopy of particle monolayer: Implications for spectral analysis of the monolayer image, Measurement 196 (2022) 111263.
[16] P. Weroński, Spectral parametrization of random particle-packings, Measurement 241 (2025) 115692.
[17] N. Thomas, P. Sreekeerthi, P. Swaminathan, Combined experimental and simulation study of self-assembly of colloidal gold nanoparticles on silanized glass, Phys. Chem. Chem. Phys. 24 (40) (2022) 25025–25035.
[18] B. Senger, J.C. Voegel, P. Schaaf, Irreversible adsorption of colloidal particles on solid substrates, Colloids Surf. A: Physicochem. Eng. Asp. 165 (1–3) (2000) 255–285.